# Calculations of the Absorption Spectrum of Chromone

**Robert Polly and Peter R. Taylor***

*San Diego Supercomputer Center and Department of Chemistry and Biochemistry, University of California, San Diego, MC 0505, La Jolla, California 92093-0505*

*Received: July 13, 1999; In Final Form: September 10, 1999*

We have performed a theoretical investigation of the optical properties of the molecule chromone, using multireference perturbation theory (CASPT2) and time-dependent density functional theory (DFT) methods. The structure of the molecule was optimized at the DFT level and at the level of complete active space self-consistent field (CASSCF). In addition to vertical excitation energies, we have computed the lowest adiabatic $^1A'$ transition energy, as well as transition probabilities for all singlet transitions to low-lying states. Using this data, we can assign the four observed ultraviolet absorption peaks of chromone. Finally, we address the question of the aromaticity of the heterocyclic ring in chromone, an issue which has recently received some attention.

## I. Introduction

Chromone ($C_7H_6O_2$, also known as benzo-$\gamma$-pyrone, Figure 1) and its derivatives are widely distributed in plant life, mostly as pigments in leaves and flowers. Despite the important role of these molecules in plant physiology, there are many open questions concerning their optical properties. Comprehensive experimental data have been obtained for the visible and ultraviolet absorption of chromone,[1−3] and the spectra show four strong absoption peaks in the 200−330 nm range. In chromone derivatives such as the anthocyanin pigments, substituent effects shift these peaks into the visible region. Although the spectra have been measured extensively, there has been no unambiguous assignment of the observed transitions to particular excitations. Studies have been performed[3−6] to address the structure and the aromaticity of chromone, but there have been no high-level ab initio calculations of the excited states of chromone to assign the spectrum. For example, in the work of Becker et al.,[3] only semiempirical methods could be used to analyze the experimental results.

It might be expected, naively, that the spectrum of chromone would be determined by $n \rightarrow \pi^*$ and $\pi \rightarrow \pi^*$ transitions. However, as we will show, the former have very small intensities, and thus the spectrum is dominated by the latter. Since the molecular symmetry is $C_s$, with all $\pi$ orbitals in the $a''$ irreducible representation, it follows that the excited states of interest to the interpretation of experiment are all $^1A'$ states. Spin−orbit coupling is expected to be small in chromone, and so transitions from the ground state to triplet excited states will be very weak. Nevertheless, the triplet states will be important in the interpretation of fluorescence spectra when these become available, and so we have also calculated the low-lying triplet states.

The complete equilibrium structure for chromone has not been determined from experiment. We have computed both the equilibrium structure and harmonic vibrational frequencies for the ground state. In order to address some issues relevant to the lowest singlet excited state of chromone, we have also optimized the geometry of this excited state, but otherwise all computed excitation energies are vertical values.

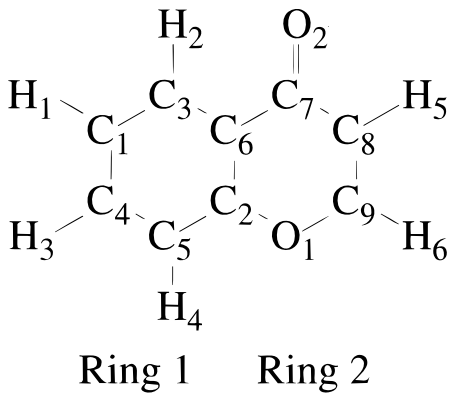


**Figure 1.** Structure of chromone. The subscripts ($C_1$, $C_2$, ..., $H_1$, $H_2$,..., $O_1$, $O_2$) in this illustration refer to the indices given in Tables 2 and 3.

There has previously been discussion of the aromaticity of chromone. The benzenoid ring is, of course, expected to have benzene-like aromaticity, but the situation with the hetero ring is less clear. Previous calculations have suggested that this ring is not aromatic, which is consistent with some of the bond lengths and angles. Our work here points more to weakly aromatic character, although of course aromaticity is not a quantum-mechanical observable and thus any definition of aromaticity is somewhat subjective. More details are presented in the body of the paper.

It is essential to use reliable methods to compute excitation spectra. The CASPT2 method[7,8] has proved extremely reliable for the prediction and analysis of spectra in a variety of organic compounds, especially ring systems, and we have used the CASPT2 method here. The feasibility of a CASPT2 study of a given system is largely determined by the CASSCF calculation that precedes it. In the case of chromone, as we shall see, we are approaching the limit of what is feasible. This means that chromone derivatives such as the anthocyanins would be beyond our current techniques. We have used our CASPT2 results to calibrate cheaper time-dependent DFT methods,[9−11] which could be applied to the anthocyanins. These methods appear to be very effective for chromone.

* To whom correspondence should be addressed.

10.1021/jp992357z CCC: $18.00 
Published on Web 11/16/1999

## II. Computational Methods

The equilibrium structure of the chromone molecule in its ground state, $X^1A'$, and the first excited state, $1^1A'$, has been optimized at the CASSCF level using Dunning's *cc*-pVDZ[12] basis set. Harmonic vibrational frequencies for the ground state were also obtained at this level. The active space for the CASSCF calculation comprised 12 orbitals: the lone pair of the $O_2$ oxygen atom (see Figure 1 for atom indices) in $a'$ symmetry and 11 $p_z$ orbitals of all carbon and oxygen atoms in $a''$ symmetry. There are 14 active electrons. The CASSCF equilibrium structures were used in the calculation of CASPT2 excitation energies. Vertical excitation energies were obtained from calculations in which several states of the appropriate symmetry were averaged in the CASSCF calculation; for the adiabatic excitation energy to the lowest $^1A'$ excited state, the orbitals were independently optimized for the ground and excited states. Transition dipole matrix elements, required to estimate intensities and oscillator strengths, were obtained at the state-averaged CASSCF level.

The chromone ground-state equilibrium structure was also optimized using DFT, with the B3LYP functional. The basis set used was a split-valence plus polarization set (SVP) augmented with a single diffuse *p* set on the non-hydrogen atoms. Following the ground-state calculation, excitation energies to both singlet and triplet states and oscillator strengths of transitions to the former were determined using DFT linear response theory: time-dependent DFT or DFT-RPA.[9−11] Two basis sets were used in these calculations: the plain SVP set mentioned above and the same basis augmented with diffuse *s* and *p* functions on the non-hydrogen atoms and diffuse *s* functions on the hydrogens. A comparison between these two sets allows us to assess the role diffuse functions play in the chromone excited states. As we will show, the effects of diffuse functions are minor in the excited states of primary interest here. Of course, the linear response treatment is appropriate only if the excitations of interest are dominated by configurations that are single excitations from the ground state, a situation which applies here.

Several methods have been proposed as a quantitative measure of aromaticity (see e.g., ref 13 for an overview). In this work, we have used the criterion of Schleyer et al.,[14−17] according to which a ring is aromatic if the absolute magnetic shielding at the geometric center of the ring is positive (and vice versa). We have calculated the shielding at the CASSCF level using London orbitals and the same *cc*-pVDZ basis used for the geometry optimization and frequency calculations.

The CASSCF geometry optimizations, frequency, and magnetic shielding calculations have been performed with the DALTON program.[18] CASPT2 calculations were performed with MOLCAS[19] and DFT-RPA calculations with Turbomole.[20] See Table 1 for a summary of the technical details of these calculations.

**TABLE 1: Technical Details of the CASSCF/CASPT2 and DFT-RPA Calculations**

| basis | *cc*-pVDZ |
|---|---|
| CASSCF Calculation | |
| roots used to average in $^1A'$ symmetry | 8 |
| roots used to average in $^1A''$ symmetry | 4 |
| roots used to average in $^3A'$ symmetry | 6 |
| roots used to average in $^3A''$ symmetry | 4 |
| CASPT2 Calculation | |
| roots calculated in $^{1,3}A'$ symmetry | 5 |
| roots calculated in $^{1,3}A''$ symmetry | 3 |
| DFT-RPA Calculation | |
| functional | B3LYP |
| basis set | VDZP |
| response | linear |

**TABLE 2: Bond Distances (Å) of the First Two States in $^1A'$ Symmetry Calculated with the CASSCF and DFT Methods**

| atom 1 | atom 2 | CASSCF $X^1A'$ | DFT $X^1A'$ | CASSCF $1^1A'$ |
|---|---|---|---|---|
| C3 | C1 | 1.386 | 1.389 | 1.438 |
| C4 | C1 | 1.408 | 1.407 | 1.427 |
| C5 | C2 | 1.403 | 1.391 | 1.422 |
| C5 | C4 | 1.387 | 1.407 | 1.433 |
| C6 | C2 | 1.394 | 1.467 | 1.443 |
| C6 | C3 | 1.410 | 1.488 | 1.431 |
| C7 | C6 | 1.482 | 1.402 | 1.457 |
| C8 | C7 | 1.469 | 1.406 | 1.474 |
| C9 | C8 | 1.344 | 1.351 | 1.343 |
| H1 | C1 | 1.081 | 1.093 | 1.080 |
| H2 | C3 | 1.080 | 1.092 | 1.078 |
| H3 | C4 | 1.081 | 1.093 | 1.079 |
| H4 | C5 | 1.080 | 1.092 | 1.078 |
| H5 | C8 | 1.079 | 1.091 | 1.079 |
| H6 | C9 | 1.078 | 1.092 | 1.078 |
| O1 | C2 | 1.358 | 1.368 | 1.348 |
| O1 | C9 | 1.345 | 1.347 | 1.353 |
| O2 | C7 | 1.210 | 1.223 | 1.217 |

## III. Results and Discussion

**A. Structure and Vibrational Frequencies.** Optimized bond lengths and bond angles obtained with CASSCF and DFT (B3LYP) are given in Tables 2 and 3. These results confirm an earlier determination of the equilibrium geometry by Somogyi.[6] Both rings retain nearly the geometry and symmetry of a benzene ring: the deviations from this geometry are only marginal. The DFT equilibrium geometry is very similar to that obtained at the CASSCF level. At the CASSCF geometry, we determined the vibrational frequencies at the CASSCF level by calculation and diagonalization of the mass-weighted nuclear Hessian. The vibrational frequencies are given in Table 4.

Perhaps the most interesting feature of the geometry and frequencies is the change in bond lengths and frequencies on excitation to the first $^1A'$ state. The C−C bonds in ring 1, the benzenoid ring, all lengthen significantly on excitation; the bonds in ring 2 are much less affected. The excited state in-plane vibrational modes, of $a'$ symmetry, have harmonic frequencies that do not differ much from their ground-state counterparts: a difference of as much as 100 $cm^{-1}$ is unusual. Conversely, the out-of-plane modes of $a''$ symmetry show much larger changes between ground and excited states with differences of more than 100 $cm^{-1}$, in modes with frequencies of only a few hundred $cm^{-1}$, being commonplace.

**B. Absorption Spectra.** The results of the calculation of the single-point excitation energies from the ground state at the equilibrium structure to the excited states in the $^{1,3}A'$ and $^{1,3}A''$ symmetries are given in Table 5. We have also calculated transition probabilities as well as excitation energies, to allow a more complete characterization of the spectrum. The transition probabilities show that the intensities of $X^1A' \rightarrow {}^1A''$ excitations will be negligible compared to the intensities of $X^1A' \rightarrow {}^1A'$ transitions. That is, the spectrum is dominated by $\pi - \pi^*$ transitions, and $n-\pi^*$ transitions are extremely weak. We can also exclude the possibility of singlet-triplet transitions in the absorption spectrum. We can therefore assign the spectrum of chromone in the 200−330 nm range to the electronic transitions $X^1A' \rightarrow N^1A'$ ($N = 1, 2, 3, 4$). As a technical detail, we may mention that the weight of the reference state is nearly constant in all CASPT2 calculations of the excited states, so there appear to be no intruder state problems in the description of the excited states.

**TABLE 3: Bond Angles (in Degrees) of the Two Lowest-Lying States in $^1A'$ Symmetry Calculated with the CASSCF and DFT Methods**

| atom 1 | atom 2 | atom 3 | CASSCF $X^1A'$ | DFT $X^1A'$ | CASSCF $1^1A'$ |
|---|---|---|---|---|---|
| C4 | C1 | C3 | 119.8 | 119.9 | 121.0 |
| H1 | C1 | C3 | 120.2 | 120.2 | 119.1 |
| H1 | C1 | C4 | 112.0 | 119.9 | 119.8 |
| C6 | C2 | C5 | 121.2 | 121.2 | 122.5 |
| O1 | C2 | C5 | 116.5 | 118.6 | 116.6 |
| O1 | C2 | C6 | 122.3 | 120.1 | 120.9 |
| C6 | C3 | C1 | 120.5 | 120.6 | 120.2 |
| H2 | C3 | C1 | 121.3 | 122.1 | 121.0 |
| H2 | C3 | C6 | 118.2 | 117.3 | 118.8 |
| C5 | C4 | C1 | 120.5 | 120.7 | 119.4 |
| H3 | C4 | C1 | 120.0 | 119.9 | 120.5 |
| H3 | C4 | C5 | 119.5 | 119.4 | 120.1 |
| C4 | C5 | C2 | 119.2 | 118.9 | 119.2 |
| H4 | C5 | C2 | 118.9 | 122.0 | 118.8 |
| H4 | C5 | C4 | 121.9 | 119.1 | 122.0 |
| C3 | C6 | C2 | 118.8 | 121.1 | 117.7 |
| C7 | C6 | C2 | 119.7 | 118.5 | 119.8 |
| C7 | C6 | C3 | 121.5 | 120.4 | 122.5 |
| C8 | C7 | C6 | 113.8 | 113.2 | 114.4 |
| O2 | C7 | C6 | 123.0 | 123.9 | 123.1 |
| O2 | C7 | C8 | 123.2 | 123.0 | 122.6 |
| C9 | C8 | C7 | 120.5 | 121.4 | 120.7 |
| H5 | C8 | C7 | 119.2 | 117.1 | 119.1 |
| H5 | C8 | C9 | 120.3 | 121.5 | 120.3 |
| H6 | C9 | C8 | 124.0 | 124.3 | 124.5 |
| O1 | C9 | C8 | 124.6 | 124.5 | 124.3 |
| O1 | C9 | H6 | 111.4 | 111.2 | 111.2 |
| C9 | O1 | C2 | 119.0 | 119.2 | 119.9 |

The ground $X^1A'$ state is dominated by a single reference configuration, and the excited states of $^1A'$ symmetry comprise linear combinations of configurations resulting from single excitations $\pi \rightarrow \pi^*$ from the ground state configuration. The excited states in $^1A''$ symmetry result from excitations from the lone pair on the $O_2$ oxygen atom into $\pi^*$ orbitals. The lowest $\pi^*$ orbitals are those of the benzenoid ring, so $n \rightarrow \pi^*$ excitations would involve significant charge transfer from the oxygen atom to the benzenoid ring. This is of low probability, as we showed above by considering the transition probabilities. The lowest-lying of the $^1A''$ states is of single-reference character, whereas the higher-lying states of this symmetry are more multiconfigurational. However, all of the important configurations (recall these are state-averaged CASSCF calculations) are again single excitations from the ground state.

The single-point excitation energies determined on the CASPT2 level do not reproduce the observed absorption maxima within the expected accuracy of 0.2 eV or better. The *cc*-pVDZ basis set is probably the smallest that could reasonably be applied to this problem, so one obvious explanation for larger than usual discrepancies between experiment and CASPT2 is the quality of the basis set. The negligible role played by diffuse functions for these low-lying excited states is discussed in more detail below. The effect of a larger sp basis or higher polarization functions would require CASPT2 calculations that are too large for us to perform because of resource limitations and technical problems. However, given that three of the four lowest excitation energies show a larger than usual difference between CASPT2 and experiment, it seems more than possible that a systematic overestimation of the excitation energies reflects shortcomings in the basis set. Another possible factor may be the effect of geometry changes in the excited states, and we have looked into this a little by reoptimizing the geometry of the first $^1A'$ excited state at the CASSCF level.

**TABLE 4: Vibrational Frequencies of Chromone in the Ground State and First Excited State ($^1A'$) at Their Equilibrium Geometries**

| ground state | | | first excited state | | |
|---|---|---|---|---|---|
| mode | irrep | $cm^{-1}$ | mode | irrep | $cm^{-1}$ |
| 1 | $a'$ | 3407.64 | 1 | $a'$ | 3413.18 |
| 2 | $a'$ | 3383.86 | 2 | $a'$ | 3402.44 |
| 3 | $a'$ | 3381.90 | 3 | $a'$ | 3393.09 |
| 4 | $a'$ | 3375.60 | 4 | $a'$ | 3384.68 |
| 5 | $a'$ | 3359.79 | 5 | $a'$ | 3378.02 |
| 6 | $a'$ | 3343.69 | 6 | $a'$ | 3361.70 |
| 7 | $a'$ | 1896.65 | 7 | $a'$ | 1843.88 |
| 8 | $a'$ | 1777.09 | 8 | $a'$ | 1830.69 |
| 9 | $a'$ | 1763.16 | 9 | $a'$ | 1747.67 |
| 10 | $a'$ | 1717.71 | 10 | $a'$ | 1707.53 |
| 11 | $a'$ | 1615.46 | 11 | $a'$ | 1650.34 |
| 12 | $a'$ | 1600.10 | 12 | $a'$ | 1539.30 |
| 13 | $a'$ | 1527.76 | 13 | $a'$ | 1521.44 |
| 14 | $a'$ | 1453.69 | 14 | $a'$ | 1499.26 |
| 15 | $a'$ | 1396.79 | 15 | $a'$ | 1435.79 |
| 16 | $a'$ | 1349.29 | 16 | $a'$ | 1373.51 |
| 17 | $a'$ | 1326.92 | 17 | $a'$ | 1314.95 |
| 18 | $a'$ | 1286.63 | 18 | $a'$ | 1275.79 |
| 19 | $a'$ | 1218.00 | 19 | $a'$ | 1232.07 |
| 20 | $a'$ | 1198.72 | 20 | $a'$ | 1161.05 |
| 21 | $a'$ | 1168.45 | 21 | $a'$ | 1103.96 |
| 22 | $a'$ | 1114.49 | 22 | $a'$ | 1079.34 |
| 23 | $a'$ | 1073.61 | 23 | $a'$ | 986.94 |
| 27 | $a'$ | 930.57 | 25 | $a'$ | 903.48 |
| 29 | $a'$ | 861.62 | 26 | $a'$ | 831.12 |
| 33 | $a'$ | 760.19 | 30 | $a'$ | 711.82 |
| 35 | $a'$ | 613.01 | 34 | $a'$ | 577.20 |
| 36 | $a'$ | 566.89 | 35 | $a'$ | 540.24 |
| 38 | $a'$ | 526.04 | 37 | $a'$ | 504.94 |
| 39 | $a'$ | 494.44 | 38 | $a'$ | 482.34 |
| 42 | $a'$ | 308.03 | 42 | $a'$ | 294.50 |
| 24 | $a''$ | 1011.50 | 24 | $a''$ | 924.16 |
| 25 | $a''$ | 986.13 | 27 | $a''$ | 813.08 |
| 26 | $a''$ | 941.49 | 28 | $a''$ | 747.95 |
| 28 | $a''$ | 891.46 | 29 | $a''$ | 729.51 |
| 30 | $a''$ | 838.97 | 31 | $a''$ | 673.45 |
| 31 | $a''$ | 790.69 | 32 | $a''$ | 648.69 |
| 32 | $a''$ | 779.84 | 33 | $a''$ | 586.44 |
| 34 | $a''$ | 698.29 | 36 | $a''$ | 530.13 |
| 37 | $a''$ | 553.12 | 39 | $a''$ | 438.03 |
| 40 | $a''$ | 481.86 | 40 | $a''$ | 396.46 |
| 41 | $a''$ | 407.22 | 41 | $a''$ | 313.98 |
| 43 | $a''$ | 254.12 | 43 | $a''$ | 206.85 |
| 44 | $a''$ | 162.58 | 44 | $al''$ | 135.20 |
| 45 | $a''$ | 116.97 | 45 | $a''$ | 120.69 |

Another alternative was to calculate the transition energy from the ground state to the first excited state in $^1A'$ symmetry at the equilibrium geometry of the first excited state. This transition energy is indeed closer to the experimental observed absorption maximum (see Table 5). But, a consideration of the ground-state energy at this geometry reveals that it is 0.13 eV above the minimum of the ground state and therefore unlikely to be populated at room temperature (this energy is approximately 5 times the thermal energy at room temperature). The values presented show that the relative positions of the ground state and the excited states allow the single-point transition energy at positions other than the two equilibrium geometries to have lower energies than the calculated one. Therefore, it can be concluded that the main reason for the large error of the calculated values is mainly that use of the single-point excitation energies is not a proper method to describe measured absorption energies of large organic molecules. An absorption peak is the convolution of many rovibrational transitions from the ground state to the excited state, and the overall shape results as a linear combination of all rovibrational transitions weighted by the

**TABLE 5: Comparison of the Absorption Maxima Determined in the Experimental Work by Becker et al.[3] and the Theoretical Results in This Work**

| Becker et al.[3] (eV) | CASPT2 (eV) | DFT-RPA (eV) | absorbing state |
|---|---|---|---|
| Geometry: Equilibrium Geometry of the Ground State $X^1A'$ | | | |
| $(1^1A')$ | 4.38 | 4.49 | $3.76 \pm 0.03$ |
| $(2^1A')$ | 4.83 | 4.96 | $4.19 \pm 0.04$ |
| $(3^1A')$ | 5.55 | 5.34 | $5.19 \pm 0.07$ |
| $(4^1A')$ | 5.57 | 5.51 | $5.77 \pm 0.08$ |
| $(5^1A')$ | 6.16 | 5.72 | |
| $(1^1A'')$ | 3.94 | 3.72 | |
| $(2^1A'')$ | 5.38 | 5.00 | |
| $(3^1A'')$ | 6.15 | 5.55 | |
| $(1^3A')$ | 3.74 | 3.26 | |
| $(2^3A')$ | 3.81 | 3.50 | |
| $(3^3A')$ | 4.19 | 4.02 | |
| $(4^3A')$ | 4.45 | 4.36 | |
| $(5^3A')$ | 5.31 | 4.84 | |
| $(1^3A'')$ | 3.70 | 3.30 | |
| $(2^3A'')$ | 5.33 | 4.87 | |
| $(3^3A'')$ | 6.10 | 5.48 | |
| Geometry: Equilibrium Geometry of the First Excited State $1^1A'$ | | | |
| $(1^1A')$ | 4.02 | – | $3.76 \pm 0.03$ |

transition probabilities and the population of the state in the ground state. Therefore, the observed absorption peak is likely to be shifted compared to the single-point electronic transition energy at the equilibrium geometries.

The results of the DFT-RPA calculations are remarkable compared to the effort required (see Table 5). The agreement with the CASPT2 results is generally to within 0.2 eV or less, at least for the lower excited states, and this is in situations where the excited states are known to be not well-described by a single configuration. The errors for the triplet states tend to be a little larger for the singlets, but, with one or two exceptions, the agreement is rather good. In view of this agreement, it seems reasonable to use the DFT-RPA approach to investigate the role diffuse functions might play in the excited states and thus whether this may be a source of error in the CASPT2 calculations. The results in Table 5 were obtained with diffuse functions added to the basis for all atoms (see Section II): deleting all the diffuse functions changes most of these excitation energies by only 0.1 eV or less. The excitation energies to the $A'$ states are systematically increased when diffuse functions are excluded, whereas the behavior of the $A''$ excitation energies is less regular. Only excitation energies in the $^1A''$ and $^3A''$ manifolds to states higher than the third are affected by more than 0.1 eV. It seems reasonable, given the agreement between the CASPT2 and DFT-RPA results, to assume that diffuse functions would play a similarly negligible role in CASPT2 calculations on the states listed.

One of the advantages of the DFT-RPA method is that it can be applied to larger systems, such as chromone derivatives, for which the active space needed for an adequate description would become so large that the calculations would be impractical. An example would be the molecule flavone (2-phenyl-chromone), another plant pigment prototype, in which $H_6$ in chromone (Figure 1) is replaced with a phenyl group. We have calculated the excitation energies to the lowest six $^1A'$ excited states in flavone using DFT-RPA in the same SVP basis, augmented with diffuse functions, as used for chromone. The geometry was obtained from an optimization at the semiempirical level (constrained to planarity). The resulting excitation energies are shown in Table 6. We may note here that for benzene itself, the lowest excited singlet states (all of which are $\pi-\pi^*$ and thus $A'$ in the subgroup that includes only the ring plane as a symmetry element) appear at excitation energies of 5.36, 6.04, and 6.98 eV at this level of treatment. It thus appears, comparing these numbers with those in Tables 6 and 5, that the lowest excited states of flavone must involve mixing between excited states in the chromone and phenyl moieties, a picture that is confirmed by the excitation structure of the solutions to the DFT-RPA equations. We emphasize that spectra at this level of treatment may be computed in a few hours of computer time on a workstation.

**TABLE 6: Excitation Energies for Flavone (2-Phenyl chromone) from DFT-RPA Calculations**

| state | excitation energy (eV) |
|---|---|
| $1^1A'$ | 4.10 |
| $2^1A'$ | 4.28 |
| $3^1A'$ | 4.55 |
| $4^1A'$ | 4.68 |
| $5^1A'$ | 4.83 |
| $6^1A'$ | 5.14 |

On the other hand, we should not overstate the capabilities of the DFT-RPA method in systems like these. Since DFT-RPA is a linear response method, it works well only when the excited states of interest are dominated by single excitations with respect to the ground-state wave function. While Hirata and Head-Gordon[21] have seen encouraging results from DFT-RPA, even in situations in which there is significant double-excitation character in the states of interest, our own experience has been much less positive. For example, in a case in which the excited state is completely dominated by a double excitation from the ground state (the lowest $^1A_g$ state in *s*-tetrazine[22]), the DFT-RPA excitation energy is 9.7 eV, more than 5 eV larger than the CASPT2 estimate. In general, the only way to be certain that DFT-RPA is applicable in a given situation seems to be to perform a calibration calculation with a method that is not limited in this way—CASPT2 is the obvious example of such a method. In the present case, since we knew from CASPT2 calculations that the lowest excited states of chromone were dominantly single excitations with respect to the ground state, the DFT-RPA method could be applied with some confidence. In addition, since the lowest states of benzene are also rather well described using DFT-RPA, we could also be rather confident that DFT-RPA would also be applicable to flavone. If suitable calibration calculations cannot be performed and the structure of the excited states of the system of interest is not known, then the DFT-RPA method must be applied with more caution.

**C. Aromaticity of the Chromone Molecule.** The aromaticity of the second ring of chromone is a long-standing question. Our calculation (see Table 7) yields a value of the absolute magnetic shielding at the geometrical center of ring 1 (the benzenoid ring) of 18.8, indicating that, as expected, this ring is aromatic. The calculated absolute magnetic shielding in the center of ring 2 is 6.7. This value is positive and therefore implies that the second ring of chromone is also aromatic. Even smaller values than this are considered to indicate aromaticity in the work of Schleyer et al.[14,15] This result is in contrast to the conclusions of an earlier theoretical study[5] based on a consideration of the molecular orbitals. However, this disagreement should not be overemphasized: the absolute shielding of ring 2 is small in magnitude, and, anyway, aromaticity is, of course, not an observable and can thus be defined in several ways that may or may not be consistent with one another. By the criterion of Schleyer and co-workers, both rings in chromone are aromatic. For completeness, we have listed shieldings at all nuclei in Table 7.

**TABLE 7: Absolute Magnetic Shieldings at the Ring Centers and at the Nuclei**

| atom | shielding (ppm) |
|---|---|
| center ring 1 | 18.8 |
| center ring 2 | 6.7 |
| C1 | 240.1 |
| C2 | 223.3 |
| C3 | 241.7 |
| C4 | 239.2 |
| C5 | 236.5 |
| C6 | 240.2 |
| C7 | 218.3 |
| C8 | 231.5 |
| C9 | 220.4 |
| H1 | 30.8 |
| H2 | 30.2 |
| H3 | 30.8 |
| H4 | 30.8 |
| H5 | 32.0 |
| H6 | 30.7 |
| O1 | 385.7 |
| O1 | 409.3 |

## IV. Conclusions

In this theoretical investigation of the chromone molecule, we have addressed three main questions—the structure of the chromone molecule, an assignment of the observed absorption spectra, and a consideration of the aromaticity of the molecule—together with a comparison of two different methods for calculating excitation spectra. An accurate theoretical description of the observed absorption spectra of chromone by means of a CASSCF/CASPT2 calculation leads to an assignment of the observed absorption maxima to the electronic transitions $X^1A' \rightarrow N^1A'$ ($N = 1, 2, 3, 4$). The accuracy of these results is not as good as would be expected: possible reasons for this were discussed in the text. Furthermore, our experience suggests that DFT-RPA (linear response) is a suitable method for the calculation of excitation energies of larger organic molecules whose ground state is well represented by a single configuration and for those excited states dominated by a single excitation from the ground state. The results obtained with this method are in good agreement with the experimental results. The DFT-RPA method can be applied to larger systems with only modest effort, as we have demonstrated by calculating also the excitation energies in flavone. Finally, we have investigated the aromaticity of the second ring of chromone. Using a criterion of aromaticity based on the sign of magnetic shielding at a ring center, we have shown that both rings of chromone are aromatic.

**Acknowledgment.** This work was supported by the Austrian Fonds zur Förderung der wissenschaftlichen Forschung in the framework of the Erwin Schrödinger Auslandsstipendium No. J1547-PHY, by the National Science Foundation through Cooperative Agreement DACI-9619020 and Grant No. CHE-9700627, and by a grant of computer time from SDSC.

## References and Notes

(1) Efimov, A. A.; Nurmuchametov, R. N.; Tolmachev, A. I. *Opt. Spectrosc.* **1970**, *29*, 6.

(2) Griffiths, P. J. F.; Ellis, G. P. *Spectrochim. Acta* **1971**, *28A*, 707.

(3) Becker, R. S.; Chakravorti, S.; Gartner, C. A.; de Graca Miguel, M. *J. Chem. Soc., Faraday Trans.* **1993**, *89*, 1007.

(4) Pereira, G. K.; Donate, P. M.; Galembeck, S. E. *J. Mol. Struct.* **1997**, *392*, 169.

(5) Ishiki, H. M.; Donate, P. M.; Galembeck, S. E. *J. Mol. Struct.* **1998**, *423*, 235.

(6) Somogyi, A.; Komáromi, I.; Dinya, Z. *Acta Chim. Hung.* **1987**, *124*, 855.

(7) Roos, B. O. *Adv. Chem. Phys.* **1987**, *69*, 399.

(8) Andersson, K.; Roos, B. O. In *Modern Electronic Structure Theory*; Yarkony, D. R., Ed.; World Scientific: Singapore, 1995; pp 55−109.

(9) Bauernschmitt, R.; Haser, M.; Treutler, O.; Ahlrichs, R. *Chem. Phys. Lett.* **1996**, *256*, 454.

(10) Bauernschmitt, R.; Ahlrichs, R. *Chem. Phys. Lett.* **1997**, *264*, 573.

(11) Casida, M. E. In *Recent Developements and Applications of Modern Density Functional Theory*; Seminario, J. M., Ed.; Elsevier: Amsterdam, 1996; p 391.

(12) Dunning, T. H. *J. Chem. Phys.* **1989**, *90*, 1007.

(13) Schleyer, P. v. R.; Jiao, H. *Pure Appl. Chem.* **1996**, *68*, 209.

(14) Schleyer, P. v. R.; Maerker, C.; Dransfeld, A.; Jiao, H.; van Eikema Hommes, N. J. R. *J. Am. Chem. Soc.* **1996**, *118*, 6317.

(15) Jiao, H.; Schleyer, P. v. R.; Mo, Y.; McAllister, M. A.; Tidwell, T. T. *J. Am. Chem. Soc.* **1997**, *119*, 7075.

(16) Jiao, H.; Schleyer, P. v. R.; Beno, B. R.; Houk, K. N.; Warmuth, R. *Angew. Chem., Int. Ed. Engl.* **1997**, *36*, 2761.

(17) Schleyer, P. v. R.; Jiao, H.; van Eikema Hommes, N. J. R.; Malkin, V. G.; Malkina, O. L. *J. Am. Chem. Soc.* **1997**, *119*, 12669.

(18) Dalton—A second-order molecular properties program, written by Helgaker, T.; Jensen, H. J.; Jørgensen, P.; Olsen, J.; Ågren, H.; Bak, K. L.; Bakken, V.; Dahle, P.; Heiberg, H.; Jonsson, D.; Kobayashi, R.; Koch, H.; Mikkelsen, K.; Norman, P.; Ruud, K.; Taylor, P. R.; Vahtras, O.

(19) Andersson, K.; Blomberg, M. R. A.; Fülscher, M. P.; Karlström, G.; Lindh, R.; Malmqvist, P. Å.; Neogrády, P.; Olsen, J.; Roos, B. O.; Sadlej, A. J.; Schuetz, M.; Seijo, L.; Serrano−Andrés, L. *MOLCAS*, version 4.0; University of Lund, Sweden, 1997.

(20) Ahlrichs, R.; Bär, M.; Baron, H.-P.; Bauernschmitt, R.; Böcker, S.; Ehrig, M.; Eichkorn, K.; Elliott, S.; Haase, F.; Häser, M.; Horn, H.; Huber, C.; Kölmel, C.; Kollwitz, M.; Ochsenfeld, C.; Öhm, H.; Schäfer, A.; Schneider, U.; Treutler, O.; von Arnim, M.; Weigend, F.; Weis, P.; Weiss, H. *TURBOMOLE*, version 4.0, University of Karlsruhe, Germany, 1996.

(21) Hirata, S.; Head-Gordon, M. *Chem. Phys. Lett.* **1999**, *302*, 375.

(22) Rubio, M.; Roos, B. O. *Mol. Phys.* **1999**, *96*, 603.